

Paris saponin II of Rhizoma Paridis – A novel inducer of apoptosis in human ovarian cancer cells

Xue Xiao^{1,2,*}, Juan Zou^{3,*}, Tri Minh Bui-Nguyen⁴, Peng Bai⁵, Linbo Gao⁶, Jinsong Liu², Shanling Liu¹, Jianguo Xiao², Xinlian Chen⁷, Xuemei Zhang⁷, He Wang^{1,**}

¹ Department of Gynecology and Obstetrics, West China Second University Hospital, Sichuan University, Chengdu, China;

² Department of Pathology, The University of Texas M. D. Anderson Cancer Center, Houston, Texas, USA;

³ Department of Pathology, West China Second University Hospital, Sichuan University, Chengdu, China;

⁴ Department of Biochemistry and Molecular Biology, The George Washington University, Washington, DC, USA;

⁵ West China School of Preclinical and Forensic Medicine, Sichuan University, Chengdu, China;

⁶ Laboratory of Molecular and Translational Medicine, West China Institute of Women and Children's Health, West China Second University Hospital, Sichuan University, Chengdu, China;

⁷ Lab of Genetics, West China Second University Hospital, Sichuan University, Chengdu, China.

Summary

Rhizoma Paridis (dried root and rhizome) has been an essential ingredient in traditional Chinese herbal medicine. In the past decade, active components of Rhizoma Paridis – the Paris saponins have emerged as promising anti-cancer agents. Among these saponins, polyphyllin D (Paris saponin (PS) I), has been extensively studied and proposed to be a potent antitumor agent. In this study, we continue to establish the efficacy and mechanisms underlying the cytotoxic effects of the steroidal PS members, namely formosanin C (PSII) in ovarian cancer treatment. We isolated PSII and evaluated its effects on a panel of ten human cell lines. Isolated PSII has potent inhibitory effects on the growth of tumor cells without deleterious effects to different normal cell types or benign neoplastic derived cells. While PSII, PSI, and etoposide are effective promoting agents for cell cycle arrest and apoptosis, PSII appeared to be marginally more potent than the later two in inhibiting SKOV3 cell growth. In PSII-treated SKOV3 cells, there was an elevation in proapoptotic elements including Bax, cytosolic cytochrome *c*, activated-caspase-3, and activated-caspase-9. The treatment also reduced extracellular signal-regulated kinase (ERK1/2) phosphorylation and anti-apoptotic Bcl-2 expression. We also assessed the antitumor efficacy of intraperitoneal administration of PSII in human SKOV3 ovarian cancer xenografts in athymic mice. PSII treatment significantly inhibited the growth of xenograft tumors relative to controls by 70% ($p < 0.05$). These findings demonstrated that, in addition to the unique selectivity against cancer cells, PSII is a potent antitumor molecule that may be developed as a cancer therapeutic agent.

Keywords: Asian medicine, cancer, Chinese/Oriental medicine, gynecology, mitogen-activated protein kinase

1. Introduction

Since ancient times, Rhizoma Paridis, a stem of *Paris polyphylla* Smith var. *chinensis* (Franch.) Hare or *Paris*

polyphylla Smith var. *yunnanensis* (Franch.) Hand.-Mazz., has been an essential ingredient of traditional Chinese medicine. Rhizoma Paridis can be found in herbal medicines used to treat diseases and conditions including microbial infection, hemorrhage, menometrorrhagia, and venomous poison (1-4). The main constituents of Rhizoma Paridis are the steroidal saponins, a family of glycosides with a chemical structure that contains either a steroid or a triterpenoid attached *via* C3 and an ether bond to a sugar side chain (5-10). Because of the crucial roles of Rhizoma Paridis in traditional herbal medicines,

* Xiao X and Zou J contributed equally to this paper.

**Address correspondence to:

Dr. He Wang, Department of Obstetrics and Gynecology, West China Second University Hospital, Sichuan University, No. 20, Block 3, Renmin Road, Chengdu 610041, China.

E-mail: wanghe_cd@126.com

the pharmacologically active components of *Rhizoma Paridis*, *i.e.*, saponins, have been isolated. Phytochemical and pharmacological studies have further unlocked a novel therapeutic role as an anticancer agent for these steroid saponins (6,11-17). Interestingly, like several other traditional herbal products that have gradually been used in conjunction with modern medicine in cancer treatment (18), evidence-based research into the mechanism underlying the cytotoxic effects of Paris saponin (PS) remains undefined.

Thirty saponins of the diosgenyl saponin (R1 = H), pennogenyl saponin (R1 = OH) and the prototype saponin sub-group have hitherto been identified from the stem of *Rhizoma Paridis* (19,20). Preliminary screening studies of the isolated saponins from the crude extract of *Rhizoma Paridis* suggested that steroidal saponins, including Paris Saponin I (PSI) and II (PSII), also known as polyphyllin D and formosanin C, respectively, exhibit comparable inhibitory effects against tumor cell growth. While PSI has been extensively studied for its ability to inhibit tumor growth (5,11,14,21,22), PSII has only recently emerged as another potential antitumor agent (22,23). Hence, as part of a concerted effort to characterize and develop active constituents of traditional herbal medicines in modern cancer treatment, in this study, we examine the mechanism underlying the cytotoxic effects of PSII and its putative antitumor properties. The effects of PSII on cell viability were examined on ten human cell lines and primary cell types. The mode of action of PSII-induced cell death was further studied using the SKOV3 cell growth model. We also assessed the efficacy of PSII in an ovarian cancer tumor-bearing mouse model. The results from our current experiments not only establish the relationship between structurally similar steroid saponins and antitumor cell proliferation activity but also provide a promising lead for the use of natural products in ovarian cancer treatment.

2. Materials and Methods

2.1. Materials

PSI and PSII were obtained from the Department of Pharmacology at Sichuan University (Chengdu, Sichuan, China). PSII was purified as previously described (19). Briefly, PSII was isolated from *Rhizoma Paridis* using a silica gel, macroporous adsorption resin, Sephadex LH-20, and RP-C18 column chromatography. The structure of PSII was determined by electrospray ionization mass spectrometry and ¹H and ¹³C nuclear magnetic resonance spectral analysis (24). Etoposide (VP16) and β-actin antibody were purchased from Sigma Chemical Co. (St. Louis, MO, USA). Primary antibodies Bcl-2, Bax, ERK1/2, phospho-ERK1/2 (Thr202/Tyr204), cytochrome *c*, caspase-3, and caspase-9 were obtained from Santa

Cruz Biotechnology Inc. (Santa Cruz, CA, USA).

2.2. Cell lines and cell culture

SKOV3, a human ovarian cancer cell line; Caski, a cervical epitheloid carcinoma cell line; A549, a human lung adenocarcinoma cell line; HepG2, a hepatocellular carcinoma cell line; SiHa, cervical carcinoma cell lines; and HEC-1A, an endometrial carcinoma cell line; all were purchased from the American Type Culture Collection (Rockville, MD, USA). An ovarian surface epithelial cell (OSE) line, human vascular smooth muscle cells, human bronchial cells, and human meningeal cells were obtained from Sichuan University, China. Cells were cultured using RPMI-1640 medium (Gibco BRL, Life Technologies Gaithersburg, MD, USA) supplemented with 10% fetal bovine serum (FBS) (HyClone, Logan, USA) at 37°C in 5% CO₂.

2.3. PSII treatment and determination of cell survivability

Cells were seeded at a density of 5×10^3 per well in 96-well tissue culture plates for 12 h prior to treatment. Carrier DMSO (< 0.1%) was used as a negative control. Viability was examined using the 3-[4, 5-dimethylthiazol-2-yl]-2, 5-diphenyltetrazolium bromide (MTT; Sigma, USA) assay (5). Dose- and time-dependent curves of PSII-treated cells were generated. The cytotoxic effects of tested agents were expressed as the 50% inhibiting concentration (IC₅₀) or total growth inhibiting concentration (TGI). SPSS software version 13.0 (SPSS Inc., China) was used to calculate IC₅₀ and TGI.

2.4. Transmission electron microscopy (TEM)

SKOV3 cells were treated with 10 μM PSII for 24 h. Harvested cells were then fixed in 5% glutaraldehyde and 3% paraformaldehyde, dehydrated in an ascending acetone series, embedded in PolyBed 812 resin, sectioned into ultra-thin longitudinal sections, and imaged using a transmission electron microscope (JEOL 1010, Jeol, Tokyo, Japan) as previously described (25).

2.5. Flow cytometry analysis

SKOV3 cells were treated with PSII at various concentrations (1 μM, 5 μM, 10 μM, and 20 μM) or with 10 μM PSII and were harvested at different time points (0, 24 h, and 48 h). Cells were labeled with propidium iodide (PI, 50 μg/mL, Sigma, USA) for 30 min at room temperature in the dark and the DNA content was determined by flow cytometry after filtration with a 300 dialyzer (FACSsort, Becton Dickinson, San Jose, CA). Cell apoptotic incidence and distribution of the cell cycle were analyzed using CellQuest software (Becton Dickinson, CA, USA)

and ModFit software (Verity Software House, USA). Experiments were conducted in triplicate.

2.6. Terminal deoxynucleotidyl transferase-mediated dUTP nick end labeling (TUNEL) assay

Cells were allowed to grow on cover slides pretreated with poly-(L)-lysine for 12 h prior to PSII treatment. The cell layers were fixed with 4% paraformaldehyde solution for 15 min at room temperature, washed with phosphate buffered saline (PBS), and then permeated with permeabilization solution (Triton X-100, 0.1% and sodium citrate) at 4°C for 2 min. SKOV3 cell samples were labeled with the TUNEL reaction mixture for 1 h at 37°C according to the manufacturer's protocol (Roche Applied Science, USA). Apoptosis was determined as the percentage of TUNEL positive cells per 1,000 DAPI-stained nuclei. Images were recorded using fluorescence microscopy (Confocal Scanning Laser Microscopy, Leica TCS4D, Germany) (26).

2.7. Western blotting analysis

SKOV3 cells were treated with PSII for 24 h. Harvested cells were collected to determine the apoptotic index and subsequently subjected to Western blot Analysis. Briefly, whole cell lysates were obtained using RIPA Buffer (Sigma, USA) and the protein concentrations were determined using the Bradford assay. Twenty five micrograms of total proteins was resolved in 12% sodium dodecyl sulfate polyacrylamide gel electrophoresis (SDS-PAGE). Proteins of interest were detected by Western blot using primary antibodies (anti-Bcl-2 (1:1,000), anti-Bax (1:3,000), anti-ERK1/2 (1:2,000), anti-phospho-ERK1/2 (Thr202/Tyr204) (1:2,000), anti-cytochrome *c* (1:2,000), anti-pro-caspase-9 (1:1,000), anti-caspase-9 (1:1,000), anti-pro-caspase-3 (1:2,000) and anti-caspase-3 (1:2,000)) and HRP-conjugated secondary antibodies. Blots were developed with enhanced chemiluminescence (ECL, Pierce, USA) and exposed to X-ray film.

2.8. Immunohistochemical analysis

PSII-treated cells were fixed with 3-aminopropyl-triethoxysilane at 60°C for 60 min. The paraffin sections were treated with 0.3% hydrogen peroxide at room temperature to block endogenous peroxidase activities and incubated with 5% bovine serum albumin to prevent nonspecific binding. Treated sections were exposed to antibodies anti-Bcl-2 (1:100), anti-Bax (1:50), anti-caspase-3 (1:100), and anti-caspase-9 (1:100). After being processed, images of the stained slides were digitized to obtain grey values using a CoolSnap Pro video camera (Meyer Instruments, Houston, TX, USA) interfaced to an Olympus BX2 microscope (Olympus, Center Valley, PA) with a 20× magnification objective.

2.9. The effect of PSII in a xenograft model of ovarian cancer

The model has been described previously (5). Briefly, 5×10^6 SKOV3 cells were injected subcutaneously into 4- to 6-week-old female BALB/c athymic nude mice (Chengdu Experimental Animal Center, Chengdu, China) and the mice were randomly divided into 6 groups ($n = 5$). PSII and PSI dosages (15 mg/kg and 25 mg/kg) and schedules were established according to preliminary toxicologic and pharmacokinetic studies and from a previous study, respectively (5). One week after implantation, treatment groups received their first doses of either PSI or PSII dissolved in a vehicle solution of DMSO (< 0.1%) and diluted in saline solution. Administrations were carried out on 4 consecutive days per week for 4 weeks (between day 8 and 35). Control groups received the vehicle (DMSO, < 0.1%) in saline solution. General clinical observations of the mice and determination of body weight and tumor growth were made twice weekly. Two perpendicular diameters of the xenograft in centimeters were measured to estimate the tumor mass using the formula $(a \times b^2)/2$. At the termination of the study, all mice were euthanized using carbon dioxide asphyxiation. All experiments were conducted based on the guidelines of The Institute for Nutritional Sciences (Shanghai, China).

2.10. Statistical analysis and reproducibility

The results were given as standard error of the mean. SPSS software version 13.0 (SPSS Inc., China) was used to calculate IC_{50} . Statistical analysis was performed using the Student's *t* test. $p < 0.05$ was considered significant.

3. Results

3.1. Treatment with PSII inhibits the growth of human tumor cell lines

Figure 1A shows the chemical structural similarity between PSI and PSII. Cell survival curves of the six cancer cell lines (A549, CASKi, SiHA, HepG2, HEC-1A, and SKOV3) after exposure to PSII (10 μ M) for 4 days show < 50% cell survival compared to nontreated groups. Specifically, the IC_{50} s for PSII in tumor derived cell lines Caski, SiHa, HEC-1A, SKOV3, A549, and HepG2 were 5.7 μ M, 3.7 μ M, 2.1 μ M, 2.4 μ M, 4.0 μ M, and 2.2 μ M, respectively. We also assessed the possibility of PSII to sensitize primary human cells from different origins and benign neoplastic derived cells. As shown in Figure 1B, the growth inhibitory property of PSII is selectively against tumor derived cells. PSII treatment did not suspend the growth of several different normal cell types including human bronchial epithelial cells, human vascular smooth muscle cells,

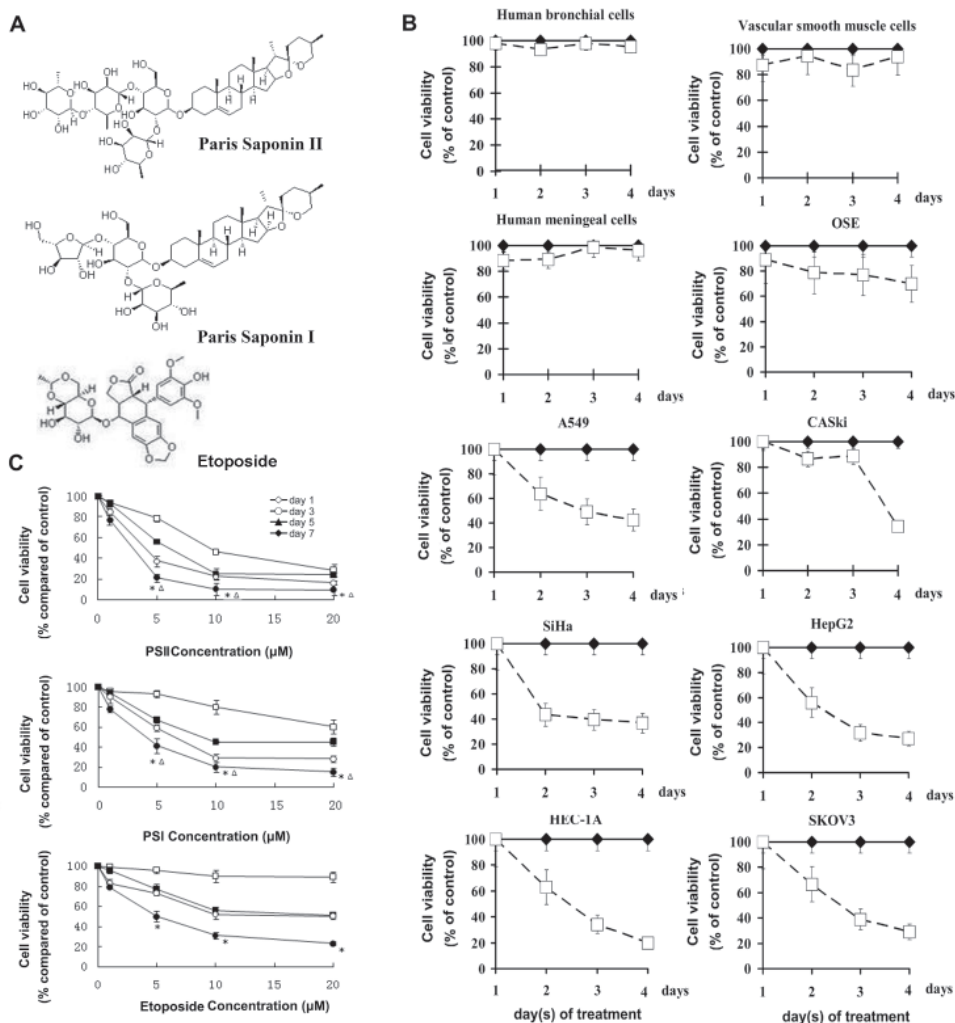


Figure 1. PSII inhibits tumor cell proliferation. (A) The structure of Paris saponin II (PSII), including an α -L-rhamnopyranosyl group at C-2 of the glucosyl moiety that plays an important role in the activity of PSII. The α -L-arabinofuranosyl and β -D-glucopyranoside at C-4 of the inner glucosyl moiety have limited roles. The chemical structure of PSI and etoposide are included. (B) Different cell lines were treated with PSII for 4 days. Cell viability was determined by MTT assay. PSII does not have any effect on the survival of normal human meningeal, human vascular smooth muscle, or human bronchial cells. PSII has marginal inhibitory effects on the growth of immortalized ovarian surface epithelial (OSE) cells. In contrast, PSII decreases cell viability of tumor derived cell lines: HEC-1A, A549, HepG2, SKOV3, Caski, and SiHa. Error bars represent standard error of the mean (SEM) ($n = 3$). (C) Dose-effect curves for PSII, PSI, and etoposide on the SKOV3 cell line for 1, 3, 5, and 7 days. * $p < 0.05$, vs. day 1 group; $\Delta p < 0.05$, vs. VP16 group.

and human meningeal cells. Interestingly, we still observed a marginal growth inhibitory effect on the immortalized OSE cell line known to develop sporadic chromosome instability (27). Since our primary interest is ovarian cancer, SKOV3, which exhibited the most sensitivity toward PSII treatment, was further studied. The kinetic study demonstrated that PSII treatment inhibits SKOV3 cell growth in a dose- and time-dependent manner. At a concentration of 10 μ M, the inhibition index of PSII after 7 days treatment was at a remarkable rate of 90.0% compared to PSI (80.3%) and etoposide (69.2%), a known cytotoxic agent. After a 24-hour treatment, the IC_{50} and TGI values of PSII on treated SKOV3 cells were 2.4 μ M and 6.3 μ M, respectively compared to those of PSI (3.1 μ M and 9.3 μ M) and etoposide (3.2 μ M and 9.7 μ M) (Figure 1C). The results demonstrate potent inhibitory effects on the

growth of tumor cells without deleterious effects on different normal cell types or benign neoplastic derived cells of PSII. However, most interestingly, while having marked structural similarities, PSII seemed to render better growth inhibitory effects than PSI on SKOV3 cells at the same concentration and time point.

3.2. Characterization of PSII-induced apoptosis in solid tumor cells

To understand the nature underlying PSII's effects on tumor cells' viability, we examined structural changes of treated SKOV3 cells. Tumor cells treated with PSII (10 μ M) displayed morphological changes as early as 4 h after initial exposure. After 12 h of PSII treatment, cells shrunk and ensued cell detachment from the culture surface at 24 h suggesting on-going induction of anoikis

(Figure 2A). Ultrastructural electron microscopy analysis of SKOV3 cells demonstrated morphological changes characteristic of apoptosis such as membrane blebbing, fragmentation with apoptotic bodies, swelling of organelles and nuclear condensation (Figure 2B). DNA fragmentation assays showed oligonucleosomal DNA ladders in PSII-treated cells (data not shown), a typical characteristic of cells undergoing apoptosis, confirming that PSII induced apoptosis in SKOV3 cells. The results were complemented by TUNEL staining studies showing

an increased percentage of TUNEL positive cells in a concentration dependent manner. Particularly, at 5 μM and 10 μM , PSII induced distinctly high percentages of TUNEL-positive cells (Figure 2C).

To further characterize cell death induced by PSII, the relative portion of DNA contents were assessed by cell cycle analysis by propidium iodide staining using flow cytometry. SKOV3 cells treated with either various concentrations (1 μM , 5 μM , 10 μM , and 20 μM) for 24 h or with 10 μM of PSII for multiple time courses (0 h,

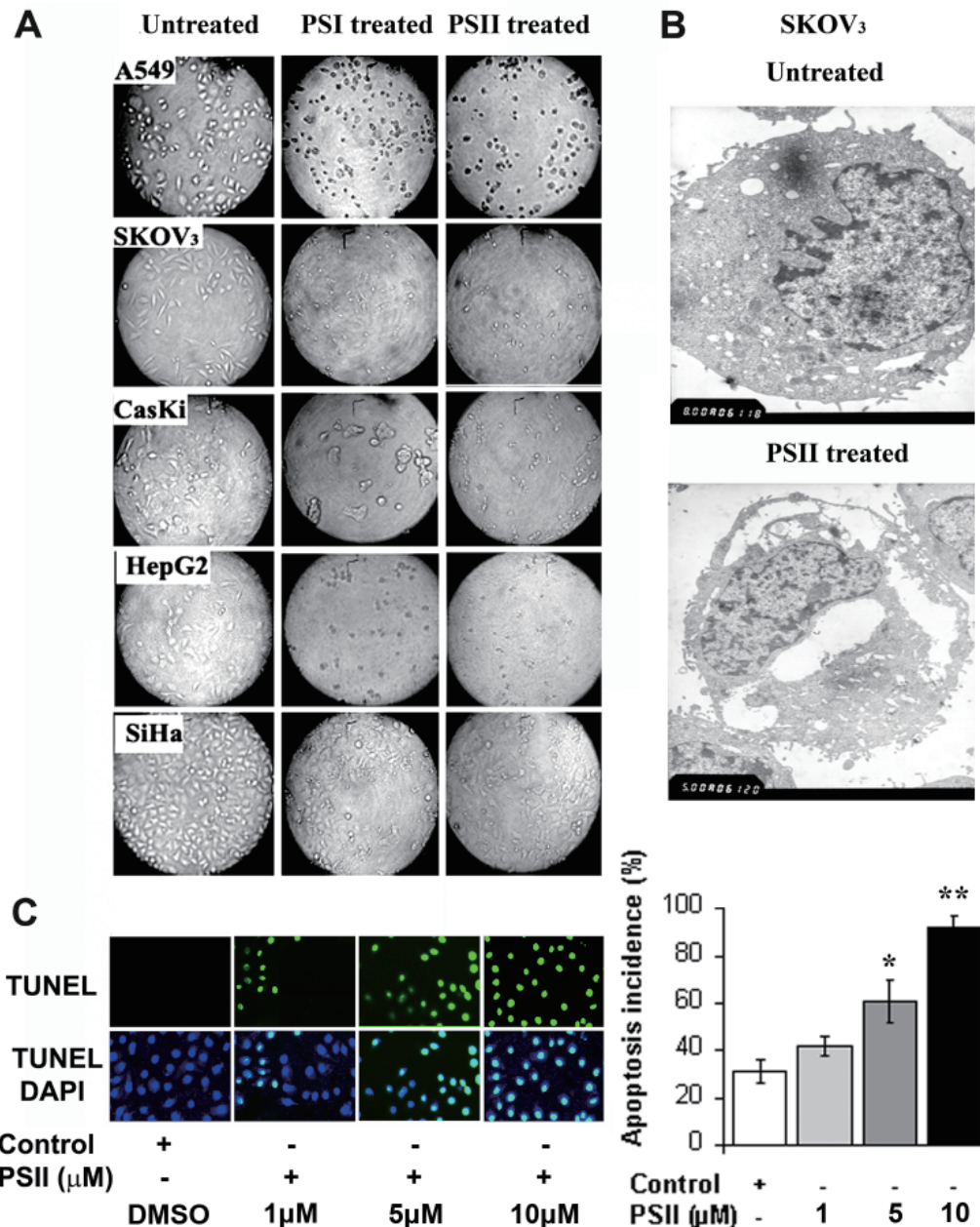


Figure 2. (A) Phase contrast images were recorded at 40 \times magnification using an Olympus BX60 upright microscope showing PSII (10 μM) and PSI (10 μM) induced morphology changes in A549, SKOV3, CasKi, HepG2, and SiHa cells after a 24 h treatment. Untreated cells (only exposed to DMSO (< 0.1%) in saline) were used as controls. (B) Transmission electron microscopy of SKOV3 cells treated with PSII (10 μM) for 24 h (lower panel). Images were recorded at 5,000 \times magnification using a transmission electron microscope. Displays show structural changes in treated cells compared to control (upper panel). (C) SKOV3 cells were treated with different concentrations of PSII and labeled with TUNEL and DAPI after 24 h. Images of random fields ($n = 10$) per slide ($n = 3$) were collected at 400 \times . Data is presented as the percentage of TUNEL positive cells (green fluorescence) per total number of treated cells (blue-DAPI staining) (* $p < 0.05$, ** $p < 0.01$, compared to control). Representative figures of treated cells labeled for TUNEL and counterstained with DAPI are shown.

24 h, 48 h, 72 h) were subjected to analysis. The results indicated PSII treatment induced SKOV3 cell death in a concentration- and time-dependent manner (Figures 3A and 3B). While concentration dependent studies showed only a marginal percentage of cell death after 24 h of PSII (10 μ M) exposure, cell cycle analysis indicated a marked increase in the cell population trapped in the G₂ phase as compared to those of the control group. However, cell death was more evident at and after 48

h of treatment (22.1% compared to 2.2% at time 0) (Figures 3C and 3D). Together, the results suggest that PSII treatment caused cell cycle arrest and apoptosis.

3.3. PSII activates the apoptotic pathway and targets ERK activity

In a previous study, PSI has been shown to activate the mitochondrial apoptotic pathway (5). Thus, to

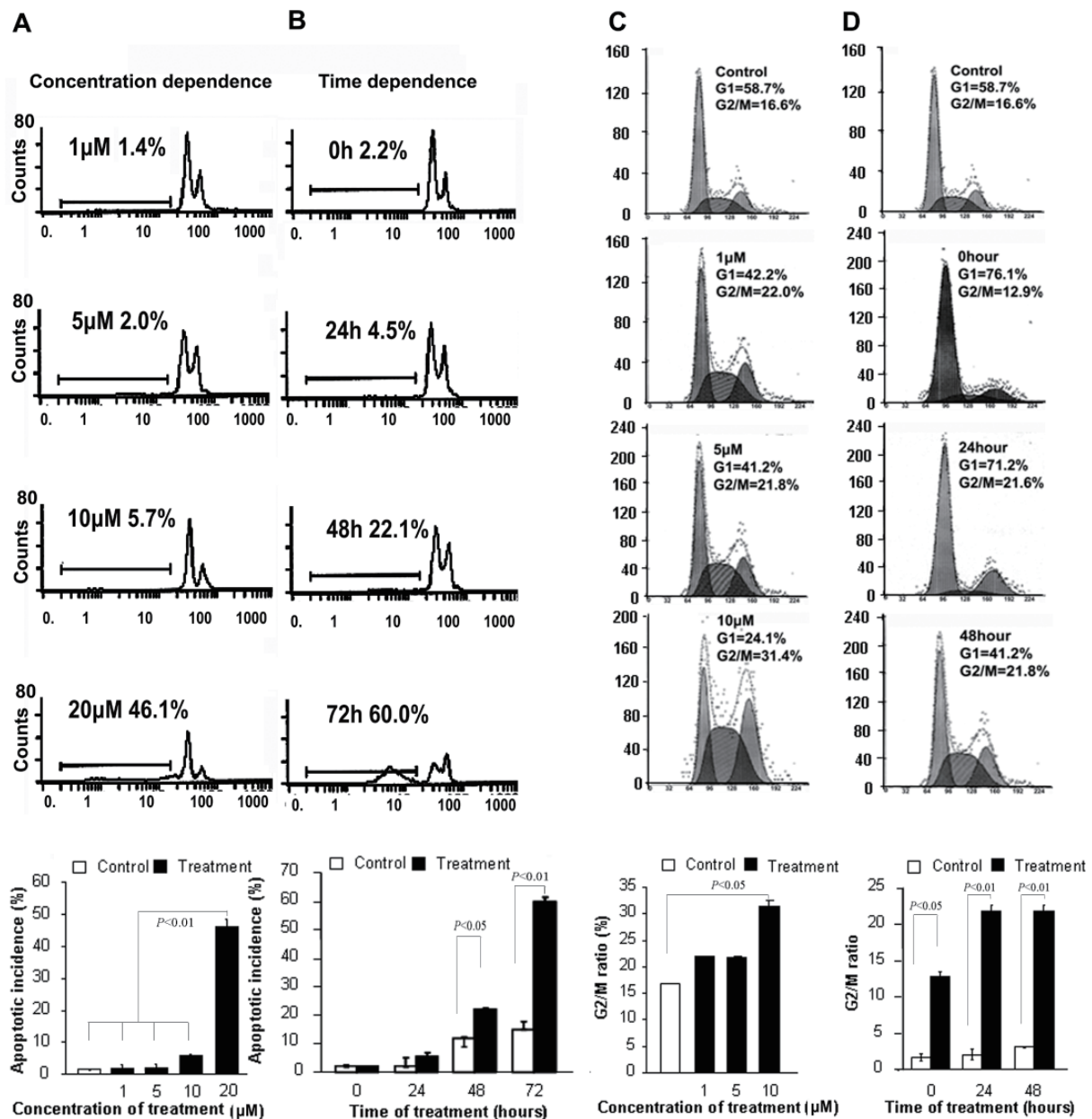


Figure 3. FACS analysis for apoptotic incidence. Special Ap peaks illustrate the characteristics of the cell population committed to apoptosis. (A) SKOV3 cells were treated with different concentrations of PSII for 24 h. The bar chart demonstrates percentage of apoptotic incidence compared to control. **(B)** SKOV3 cells were treated with PSII (10 μ M) and were analyzed for percentage of apoptotic incidence at different time points. The bar chart summarizes the results as percentage of apoptotic incidence compared to control. **(C)** PSII induces G₂/M phase arrest in SKOV3 cells in a concentration dependent manner. The SKOV3 cells were treated with different concentrations of PSII (0, 1 μ M, 5 μ M, and 10 μ M) for 24 h and subsequently labeled with propidium iodide staining and analyzed using fluorescence-activated cell sorting analysis. The bar chart summarizes the results as percentage of cells in the G₂/M phase. **(D)** PSII induces G₂/M phase arrest in SKOV3 cells. SKOV3 cells were cultured with or without PSII (10 μ M) for 0, 24 h, and 48 h. All treated cells were stained with propidium iodide and analyzed using fluorescence-activated cell sorting analysis. The bar chart shows the percentage of cells in the G₂/M phase. Error bars represent standard error of the mean (SEM) ($n = 3$) ($p < 0.05$ and $p < 0.01$, compared to control to be considered as significant).

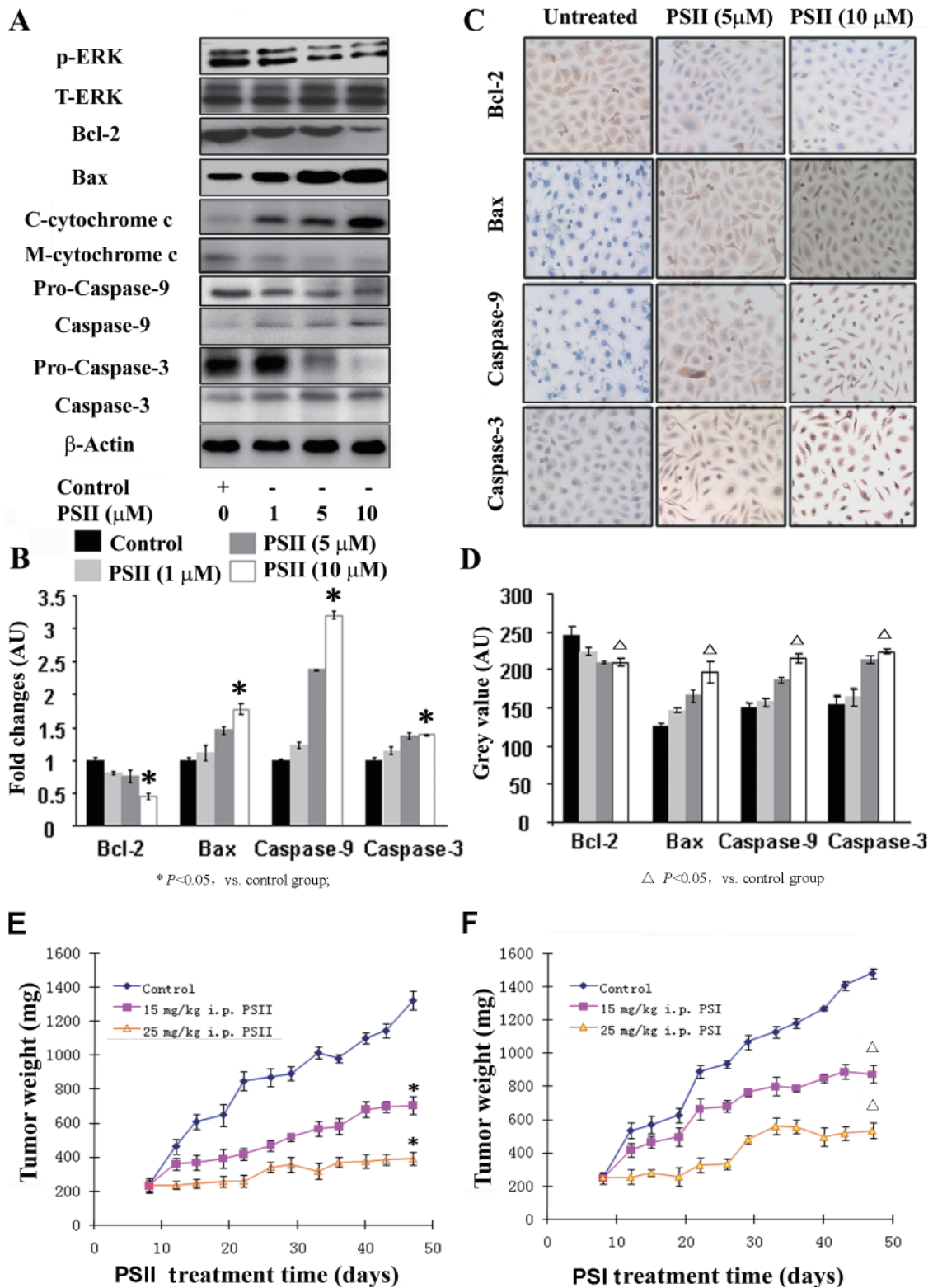


Figure 4. PSII induces caspase activation and cytochrome *c* release and inhibits ERK1/2 phosphorylation in treated SKOV3 cells. (A) Western blot analysis for SKOV3 cells treated with different concentrations of PSII for 24 h. DMSO (< 0.1%) diluted in saline was used as a control. β-Actin was used as a loading control. M-cytochrome *c*-mitochondrial cytochrome *c* and C-cytochrome *c*-cytosolic cytochrome *c*. (B) Densitometric analysis was performed for Bcl-2, Bax, active caspase-9, and active caspase-3. Values were normalized to β-actin, * *p* < 0.05, compared to control. (C) Sections were analyzed by immunohistochemistry for Bax, Bcl-2, caspase-3, and caspase-9. (D) Quantification using immunohistochemical staining for Bax, Bcl-2, caspase-3, and caspase-9. Data are presented in arbitrary values (*n* = 3, ^Δ *p* < 0.05, compared to control). (E and F) Paris saponins (PSI and PSII) inhibit tumor growth in a xenograft model of ovarian cancer. Mice were implanted with 5 × 10⁶ SKOV3 cells on day 0 and were randomly divided into various treatment and control groups (*n* = 5). Eight days after implantation, tumor-bearing mice were treated according to the protocols. Briefly, tumor-bearing mice were treated with PSI, PSII, or received the vehicle (DMSO, < 0.1%) in saline solution by intraperitoneal administration for 4 weeks, 4 consecutive days per week with two different doses of either PSI or PSII, 15 mg/kg or 25 mg/kg. Columns, mean; bars, S.D., * *p* < 0.05, ^Δ *p* < 0.05, compared to control.

understand the nature of PSII-induced apoptosis on SKOV3 cells, we examined changes in the constituents of the mitochondrial apoptotic pathway. As shown in Figure 4, 24 h PSII treatment led to the expression of proapoptotic protein Bax and the activation of apoptotic proteins such as caspase-3 and caspase-9 in a concentration manner evident by a gradual disappearance of intact pro-caspase-9 and pro-caspase-3 and appearance of proteolytic cleavage bands (Figures 4A and 4B). We also detected increased levels of cytosolic cytochrome *c* and decreased levels of mitochondrial cytochrome *c* in a concentration dependent manner. In contrast, anti-apoptotic Bcl-2 protein levels were markedly reduced in cells being treated with PSII at a concentration as low as 5 μ M. Immunochemical studies also confirmed similar observations showing that PSII treatment reduced Bcl-2 expression levels while promoting the expression of Bax and the activation of caspase-3 and caspase-9 (Figures 4C and 4D). Since inhibition of the mitogen-activated protein kinase pathway (MAPK pathway) has been shown to be associated with induction of apoptosis in tumor cells with growth inhibition (28-30), to determine whether PSII treatment inhibits tumor cell growth by modulating survival signaling, we also examined the activation status of ERK1/2. As we expected, although PSII treatment did not alter the expression levels of total ERK1/2, prominent reduction of phosphorylated ERK1/2 was observed as we increased the exposure concentration of PSII from 1 μ M to 10 μ M.

3.4. PSII inhibits tumor growth in a xenograft mouse model

To further characterize the antitumor properties of PSII, we assessed its antitumor efficacy in a well established xenograft mouse model of ovarian cancer. Both PSI and PSII did not induce any apparent acute toxic effects in treated mice. Most intriguing, as shown in Figure 4E, PSI and PSII treatment significantly delayed tumor growth. As we have shown that although both PSI and PSII have the same range of efficacy, PSII appeared to be marginally more potent than PSI. We observed the same pattern in the *in vivo* study. At the termination of the experiment, we found that intraperitoneal administration of PSII and PSI at 15 mg/kg and 25 mg/kg dosages led to a 46% and 70% and a 40% and 64% tumor growth inhibition, respectively, compared with that in control mice treated with vehicle solution of DMSO (< 0.1%) diluted in saline solution ($p < 0.05$). However, at a dosage of 15 mg/kg, the antitumor effect of PSII appeared to reach a plateau after 26 days of treatment despite the additional 2 cycles of treatment. In contrast, at the higher dosage (25 mg/kg), the additional cycles of treatment seemed to be beneficial as PSII inhibited 70% tumor growth at day 47 compared to 60% at day 26.

4. Discussion

In attempting to characterize the antitumor effects of active constituents of traditional herbal medicine with diverse therapeutic potential, PSII was isolated from *Rhizoma Paridis* and characterized (31,32). At the time of this writing, eleven steroidal saponins of *Rhizoma Paridis* have been identified, namely Paris V (3-*O*-Rha(1 \rightarrow 2)-Glc), polyphyllin C (3-*O*-Rha(1 \rightarrow 3)-Glc), PSI-polyphyllin D (3-*O*-Rha(1 \rightarrow 2)[Ara(1 \rightarrow 4)]-Glc) (14,33-36), PSII-formosanin C (3-*O*-Rha(1 \rightarrow 4)-Rha(1 \rightarrow 4)[Rha(1 \rightarrow 2)]-Glc), prosapogenin B of diosgenin (3-*O*-Rha(1 \rightarrow 4)-Glc), Paris saponin V (PSV) (3-*O*-Rha(1 \rightarrow 3)[Ara(1 \rightarrow 4)]-Glc), Paris saponin VI (PSVI) (3-*O*-Rha(1 \rightarrow 4)[Ara(1 \rightarrow 3)]-Glc), Paris saponin III (3-*O*-Rha(1 \rightarrow 4)[Ara(1 \rightarrow 2)]-Glc), gracillin (3-*O*-Rha(1 \rightarrow 2)[Glc(1 \rightarrow 3)]-Glc), polyphyllin E (3-*O*-Rha(1 \rightarrow 2)-Rha(1 \rightarrow 4)[Rha(1 \rightarrow 3)]-Glc), and polyphyllin F (3-*O*-Rha(1 \rightarrow 4)-Rha(1 \rightarrow 3)[Glc(1 \rightarrow 2)]-Rha) (3,37). Over the past few decades, the therapeutic properties of the diosgenin-steroid saponins subgroup have been explored for treatments against metabolic diseases, including hypercholesterolemia, dyslipidemia, diabetes and obesity, inflammation, and cancer (38). However, the field investigating the antitumor properties of Paris saponin has only become more active in the past five years. Multiple model systems ranging from murine lung adenocarcinoma (22), human colon adenocarcinoma grade II (17), mouse lung adenocarcinoma (23) to zebrafish embryos have demonstrated that several Paris saponins can induce programmed cell death, inhibit cell migration, and inhibit tumor cell growth. Studies from our laboratories have also unraveled PSI mechanisms of action on ovarian cancer cells (5,24,33,36,39). While PSII and PSI have remarkable chemical structural similarity, very few studies have been conducted to explore the efficacy and mechanisms underlying the cytotoxic effects of PSII in cancer treatment.

In the present study, we examined the underlying mechanism of action and the antitumor effects of PSII in ovarian cancer cells because they are not completely defined. We also attempted to develop PSII as a systemic treatment strategy for ovarian cancer that remains the fifth-leading cause of death by cancer in the developed world and the most deadly of the gynecologic malignancies (40). Here, we showed that PSII selectively inhibits growth of tumor cell lines but not non-neoplastic derived cell lines or normal cell types with relative low IC_{50} s compared with those of PSI. Similar to PSI, PSII appeared to be a more powerful cytotoxic agent than etoposide. Cytotoxic and inhibitory effects of PSII were time- and dose-dependent. Increased concentrations of PSII ensued showing increased levels of cell death signaling evident by DNA fragmentation, the activation of caspase-9 and caspase-3, and reduced levels of active ERK1/2 in treated cells.

PSII treatment also altered the expression levels of anti-apoptotic Bcl-2 and pro-apoptotic protein Bax. Both Bax and Bcl-2 are among the important regulators of cytochrome *c* release from mitochondria; the reduction of Bcl-2 levels promotes cytochrome *c* release, leading to the activation of programmed cell death. It is well known that cross-talk between Bcl-2 and Bax is intimately linked to the fate of the cell; Bax may block Bcl-2 activity and *vice versa*; however, in certain instances, Bcl-2 and Bax function independently to regulate cell death in an exclusive manner. Data from the present studies seem to suggest that PSII induced apoptotic cell death by modulating the expression of both Bcl-2 and Bax. While further studies will be necessary, the dramatic changes in Bcl-2 expression levels corroborated with other clues suggesting PSII may induce ER stress-induced cell death. The first clue was evident from the occurrence of several downstream signals upon PSII treatment such as the collapse of mitochondrial potential (data not shown) and the release of cytochrome *c*. ER stress often triggers release of Ca^{2+} and induces activation of the apoptotic pathway involving collapse of mitochondrial potential, permeabilization of the inner membrane and release of cytochrome *c* (41). Another clue came from an observation that increased concentrations of PSII in SKOV3 cell treatment resulted in the upregulation of C/EBP homologous transcription factor (CHOP) protein levels (unpublished data). CHOP is known to regulate ER stress-induced cancer cell death (33) and suppress Bcl-2 expression levels leading to a severe irremediable endoplasmic reticulum stress (42,43). Here, PSII treatment induced Bax expression in parallel with the dramatic reduction of Bcl-2 expression in PSII-treated tumor cells. While future studies will further determine the nature of PSII-induced apoptosis in ovarian cancer tumor cells, data from the present studies suggest that PSII treatment affects the mitochondrial apoptotic pathways. Indeed, these findings are supported by a study by Lee *et al.* showing PSII-formosanin C induces mitochondria membrane potential collapse and the activation of essential components of the intrinsic apoptosis pathway (17).

In addition to activating the apoptotic pathway, PSII also exerts its effect on ERK MAPK. The activation of the MAP-ERK pathway often stimulates cell differentiation, mitosis, and hypertrophy (44). In cancer, key events in the cellular transformation process such as proliferation, migration, and tumor development have been linked to the activation of ERK1/2 signaling and its role in relaying communication between growth factor receptors and the cell nucleus (45). ERK MAPK also phosphorylates caspase-9 at Thr125 resulting in the inhibition of caspase-9 processing and caspase-3 activation (46). Therefore, the effects of PSII treatment on ERK MAPK activation in a dose-dependent manner accompanied with increased levels of activated caspases

further suggests that PSII elicits its inhibitory effects *via* modifying ERK activities.

We also demonstrated that PSII has a potent antitumor activity. In a comparative study (23), PSII appears to be more effective in inhibiting tumor growth and pulmonary metastasis than cisplatin in a T739 bearing LA795 cells mice. Interestingly, this study also showed that PSII appeared to be marginally more potent than PSI, especially, at the higher dosage (25 mg/kg). It appears that at the higher dosage (25 mg/kg), the additional cycles of treatment seemed to be beneficial compared to the PSI treatment. These results offer an interesting observation that may allow us to develop a strategy for a proper schedule for the administration of PSI and PSII as single agent or in adjuvant therapy. Of note, while *Rhizoma Paridis* has been used for thousands of years, it is also reasonable to assume that the bioactivity of *Rhizoma Paridis* is a synergistic effect of multiple active constituents including PSI and PSII.

In conclusion, we have shown that PSII targets tumor cells *via* multiple mechanisms including modulating ERK1/2 activity, inducing cell-cycle arrest, and activating the mitochondrial apoptotic pathway. While the chemical structure of PSI and PSII are markedly similar, the relative higher potency of PSII suggests that further investigations into their structure-functions and associated biological effects may have value for improving the effectiveness of an anti-cancer strategy in a clinical setting.

Acknowledgements

We would like to thank Dr. Hao Zhang and Dr. Hongxiang Yin for PSI, PSII, and PSVI compounds. We also thank Diane Hackett and Maude E. Veech for technical support. This work was supported by the Fund of National Nature Science Foundations (Grant No. 81001159/30571942/C03030401), and National Research Foundation for the Doctoral Program of Higher Education of China (Grant No. 20020610089).

References

1. Vassilopoulos Y. *Paris polyphylla* in medicine. A literary favour to world culture. Newsfinder. 2008.
2. Wang Q, Cheng YB. The bacteriostasis and hermostasis functions of *Paris polyphylla* Smith var. *Chinensis* (French.) Hera. The Journal of China Pharmaceutical University. 1989; 20:251-253. (in Chinese)
3. Harborne JB. Saponins used in traditional and modern medicine and Saponins Used in Food and Agriculture. *Phytochemistry*. 1997; 46:1301-1303.
4. XC ZX. The study and application of Paris plant. *Journal of Chinese Herbal Technology*. 2000; 7:346-347. (in Chinese)
5. Xiao X, Bai P, Bui Nguyen TM, Xiao J, Liu S, Yang G, Hu L, Chen X, Zhang X, Liu J, Wang H. The antitumoral effect of Paris saponin I associated with the induction of apoptosis through the mitochondrial pathway. *Mol*

- Cancer Ther. 2009; 8:1179-1188.
6. Yan L, Gao W, Zhang Y, Wang Y. A new phenylpropanoid glycosides from *Paris polyphylla* var. *yunnanensis*. *Fitoterapia*. 2008; 79:306-307.
 7. Wang Y, Gao WY, Zhang TJ, Guo YQ. A novel phenylpropanoid glycosides and a new derivation of phenolic glycoside from *Paris polyphylla* var. *yunnanensis*. *Chin Chem Lett*. 2007; 18:548-550.
 8. Wang Y, Gao WY, Liu XQ, Zuo YT, Chen HX, Duan HQ. Antitumor constituents from *Paris polyphylla*. *Asian J Tradit Med*. 2006; 1:7-10.
 9. Cheng ZX, Liu BR, Qian XP, Ding YT, Hu WJ, Sun J, Yu LX. Proteomic analysis of anti-tumor effects by *Rhizoma Paridis* total saponin treatment in HepG2 cells. *J Ethnopharmacol*. 2008; 120:129-137.
 10. Man S, Gao W, Zhang Y, Yan L, Ma C, Liu C, Huang L. Antitumor and antimetastatic activities of *Rhizoma Paridis* saponins. *Steroids*. 2009; 74:1051-1056.
 11. Wang Y, Zhang YJ, Gao WY, Yan LL. Anti-tumor constituents from *Paris polyphylla* var. *yunnanensis*. *Zhongguo Zhong Yao Za Zhi*. 2007; 32:1425-1428.
 12. Zhou J. Bioactive glycosides from Chinese medicines. *Mem Inst Oswaldo Cruz*. 1991; 86 (Suppl 2):231-234.
 13. Sun J, Liu BR, Hu WJ, Yu LX, Qian XP. *In vitro* anticancer activity of aqueous extracts and ethanol extracts of fifteen traditional Chinese medicines on human digestive tumor cell lines. *Phyther Res*. 2007; 21:1102-1104.
 14. Lee MS, Yuet-Wa JC, Kong SK, Yu B, Eng-Choon VO, Nai-Ching HW, Chung-Wai TM, Fung KP. Effects of polyphyllin D, a steroidal saponin in *Paris polyphylla*, in growth inhibition of human breast cancer cells and in xenograft. *Cancer Biol Ther*. 2005; 4:1248-1254.
 15. Chiang HC, Wang JJ, Wu RT. Immunomodulating effects of the hydrolysis products of formosanin C and beta-ecdysone from *Paris formosana* Hayata. *Anticancer Res*. 1992; 12:1475-1478.
 16. Wu RT, Chiang HC, Fu WC, Chien KY, Chung YM, Horng LY. Formosanin-C, an immunomodulator with antitumor activity. *Int J Immunopharmacol*. 1990; 12:777-786.
 17. Lee JC, Su CL, Chen LL, Won SJ. Formosanin C-induced apoptosis requires activation of caspase-2 and change of mitochondrial membrane potential. *Cancer Sci*. 2009; 100:503-513.
 18. Liu J, Li X, Liu J, Ma L, Li X, Fønnebø V. Traditional Chinese medicine in cancer care: A review of case reports published in Chinese literature. *Forsch Komplementmed*. 2011; 18:257-263.
 19. Yin HX, Xue D, Bai N, Chen C, Chen Y, Zhang H. Isolation and identification of major steroidal saponins of *Paris polyphylla* Smith var *stenophylla* Franch. *Sichuan Da Xue Xue Bao Yi Xue Ban*. 2008; 39:485-488. (in Chinese)
 20. Liu XX, Wang L, Chen XQ, Deng XT, Cao Y, Wang Q. Simultaneous quantification of both triterpenoid and steroidal saponins in various Yunnan Baiyao preparations using HPLC-UV and HPLC-MS. *J Sep Sci*. 2008; 31:3834-3846.
 21. Ma DD, Lu HX, Xu LS, Xiao W. Polyphyllin D exerts potent anti-tumour effects on Lewis cancer cells under hypoxic conditions. *J Int Med Res*. 2009; 37:631-640.
 22. Shuli M, Wenyuan G, Yanjun Z, Chaoyi M, Liu Y, Yiwen L. *Paridis* saponins inhibiting carcinoma growth and metastasis *in vitro* and *in vivo*. *Arch Pharm Res*. 2011; 34:43-50.
 23. Man S, Gao W, Zhang Y, Liu Z, Yan L, Huang L, Liu C. Formosanin C-inhibited pulmonary metastasis through repression of matrix metalloproteinases on mouse lung adenocarcinoma. *Cancer Biol Ther*. 2011; 11:592-598.
 24. Zhang XF, Cui Y, Huang JJ, Zhang YZ, Nie Z, Wang LF, Yan BZ, Tang YL, Liu Y. Immuno-stimulating properties of diosgenyl saponins isolated from *Paris polyphylla*. *Bioorg Med Chem Lett*. 2007; 17:2408-2413.
 25. Boraks G, Tampelini FS, Pereira KF, Chopard RP. Effect of ionizing radiation on rat parotid gland. *Braz Dent J*. 2008; 19:73-76.
 26. Gavrieli Y, Sherman Y, Ben-Sasson SA. Identification of programmed cell death in situ *via* specific labeling of nuclear DNA fragmentation. *J Cell Biol*. 1992; 119:493-501.
 27. Maeda T, Tashiro H, Katabuchi H, Begum M, Ohtake H, Kiyono T, Okamura H. Establishment of an immortalised human ovarian surface epithelial cell line without chromosomal instability. *Br J Cancer*. 2005; 93:116-123.
 28. Nguyen TT, Tran E, Nguyen TH, Do PT, Huynh TH, Huynh H. The role of activated MEK-ERK pathway in quercetin-induced growth inhibition and apoptosis in A549 lung cancer cells. *Carcinogenesis*. 2004; 25:647-659.
 29. Cusimano A, Foderà D, D'Alessandro N, Lampiasi N, Azzolina A, Montalto G, Cervello M. Potentiation of the antitumor effects of both selective cyclooxygenase-1 and cyclooxygenase-2 inhibitors in human hepatic cancer cells by inhibition of the MEK/ERK pathway. *Cancer Biol Ther*. 2007; 6:1461-1468.
 30. Kunnimalaiyaan M, Ndiaye M, Chen H. Apoptosis-mediated medullary thyroid cancer growth suppression by the PI3K inhibitor LY294002. *Surgery*. 2006; 140:1009-1014; discussion 1014-1015.
 31. Wei J. Determination of steroidal saponins in *Rhizoma Paridis* by RP-HPLC. *Yao Xue Xue Bao*. 1998; 33:465-458. (in Chinese)
 32. Huang Y, Cui LJ, Liu WN, Wang Q. Quantitative analysis of steroidal saponins in Chinese material medica *Rhizoma Paridis* by HPLC-ELSD. *Zhongguo Zhong Yao Za Zhi*. 2006; 31:1230-1233. (in Chinese)
 33. Cheung JY, Ong RC, Suen YK, Ooi V, Wong HN, Mak TC, Fung KP, Yu B, Kong SK. Polyphyllin D is a potent apoptosis inducer in drug-resistant HepG2 cells. *Cancer Lett*. 2005; 217:203-211.
 34. Deng S, Yu B, Hui Y, Yu H, Han X. Synthesis of three diosgenyl saponins: Dioscin, polyphyllin D, and balanitin 7. *Carbohydr Res*. 1999; 317:53-62.
 35. Li B, Yu B, Hui Y, Li M, Han X, Fung KP. An improved synthesis of the saponin, polyphyllin D. *Carbohydr Res*. 2001; 331:1-7.
 36. Siu FM, Ma DL, Cheung YW, Lok CN, Yan K, Yang Z, Yang M, Xu S, Ko BC, He QY, Che CM. Proteomic and transcriptomic study on the action of a cytotoxic saponin (Polyphyllin D): Induction of endoplasmic reticulum stress and mitochondria-mediated apoptotic pathways. *Proteomics*. 2008; 8:3105-3117.
 37. Man S, Gao W, Zhang Y, Huang L, Liu C. Identification of chemical constituents in *Rhizoma Paridis* saponins and their oral administration in rat plasma by UPLC/Q-TOF/MS. *Biomed Chromatogr*. 2011; 25:712-719.
 38. Raju J, Patlolla JM, Swamy MV, Rao CV. Diosgenin, a steroid saponin of *Trigonella foenum-graecum* (Fenugreek), inhibits azoxymethane-induced aberrant

- crypt foci formation in F344 rats and induces apoptosis in HT-29 human colon cancer cells. *Cancer Epidemiol Biomarkers Prev.* 2004; 13:1392-1398.
39. Weizhen K. Identification and clinical application of Paris Polyphylla and Bistort. *Journal of China Traditional Chinese Medicine Information.* 2010; 2:108-109.
40. Westgren M. Prevention of ovarian cancer – let's do something. *Acta Obstet Gynecol Scand.* 2012; 91:1009-1010.
41. Wu J, Kaufman RJ. From acute ER stress to physiological roles of the Unfolded Protein Response. *Cell Death Differ.* 2006; 13:374-384.
42. Oyadomari S, Mori M. Roles of CHOP/GADD153 in endoplasmic reticulum stress. *Cell Death Differ.* 2004; 11:381-389.
43. McCullough KD, Martindale JL, Klotz LO, Aw TY, Holbrook NJ. Gadd153 sensitizes cells to endoplasmic reticulum stress by down-regulating Bcl2 and perturbing the cellular redox state. *Mol Cell Biol.* 2001; 21:1249-1259.
44. Provot S, Nachtrab G, Paruch J, Chen AP, Silva A, Kronenberg HM. A-raf and B-raf are dispensable for normal endochondral bone development, and parathyroid hormone-related peptide suppresses extracellular signal-regulated kinase activation in hypertrophic chondrocytes. *Mol Cell Biol.* 2008; 28:344-357.
45. Svensson S, Jirstrom K, Ryden L, Roos G, Emdin S, Ostrowski MC, Landberg G. ERK phosphorylation is linked to VEGFR2 expression and Ets-2 phosphorylation in breast cancer and is associated with tamoxifen treatment resistance and small tumours with good prognosis. *Oncogene.* 2005; 24:4370-4379.
46. Allan LA, Morrice N, Brady S, Magee G, Pathak S, Clarke PR. Inhibition of caspase-9 through phosphorylation at Thr 125 by ERK MAPK. *Nat Cell Biol.* 2003; 5:647-654.

(Received February 24, 2012; Revised July 3, 2012; Accepted July 3, 2012)